Supporting Information

Photoreduction of CO_2 using $[Ru(bpy)_2(CO)L]^{n+}$ catalysts in biphasic solution / supercritical CO_2 systems.

Patrick Voyame, Kathryn E. Toghill, Manuel A. Méndez[†] and Hubert H. Girault*

Laboratoire d'Electrochimie Physique et Analytique, Ecole Polytechnique Fédérale de Lausanne, Station 6, CH-1015 Lausanne, Switzerland

*** Corresponding Author:**

Fax: (+)41 21 6933667

E-mail: hubert.girault@epfl.ch

1. Description of high pressure setup

The experimental setup used for all experiment is presented in Scheme S1. The reactor consist of a 32 ml stainless steel reactor equipped with a sapphire windows, water circulation inside the wall for temperature control, gas inlet and outlet and a thermocouple for temperature monitoring. Two autoclaves were used to decompress the system, the first one mainly acting as a liquid trap, the second as a sampler for gas chromatography analysis.

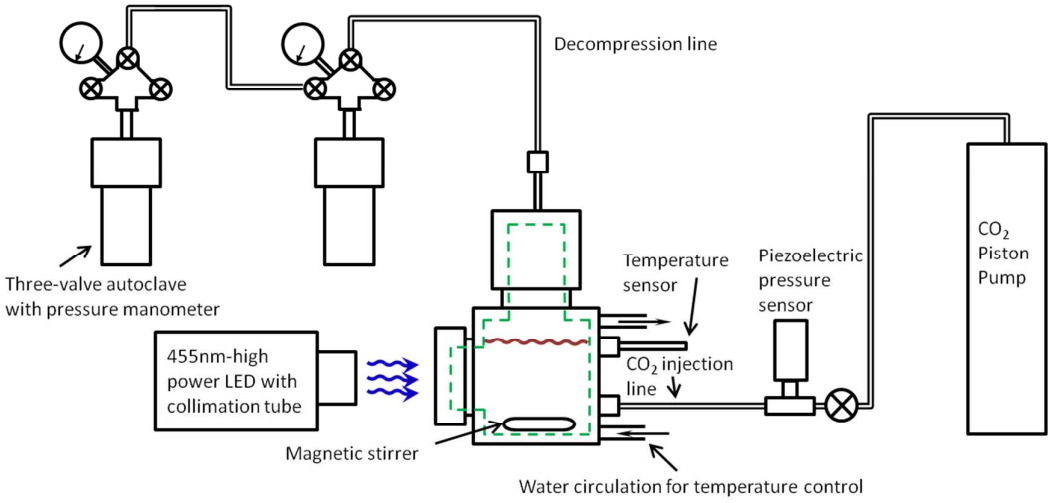

Scheme S1. *Representation of the experimental setup, the volume highlighted by the green dashed line is the inner volume of the reactor, half of this volume is filled by the solution, the interface is above the window ensuring total light absorption.*

2. Ionic chromatography analysis procedure

Analysis of the liquid phase was performed immediately after decompression of the reactor. In all experiments, a 100 µl sample was withdrawn from the reactor before sealing it, this sample was kept aside during reaction time, and analyzed by ionic chromatography to subtract the amount of formate initially present in the dimethylformamide. All samples were diluted 10 fold for analysis, to avoid overlapping of signals on the chromatogram. This dilution step was performed right before injection to avoid further degradation of the organic solvent into formic acid. Indeed DMF/H_2O mixtures are known to spontaneously produce formate especially for mixtures of high water content. This production is favoured in presence of organic bases such as TEOA or TEA.[1] As BNAH was preferred as electron donor in our experiments, the amount of formate quantified after reaction was solely attribute to

CO_2 reduction. Reactions without catalyst and photosensitizer or without light did not produce formate over 2 hours of reaction confirm that the formate detected is produced by degradation of the dimethylformamide.

A typical chromatogram obtain after reaction is shown in Figure S1, with identification of the different peaks. The calibration curve used for quantification is also shown. All measurements for this calibration were performed in the same DMF/water mixture, the amount of formate originally present in the solvent mixture was subtracted for every measurement.

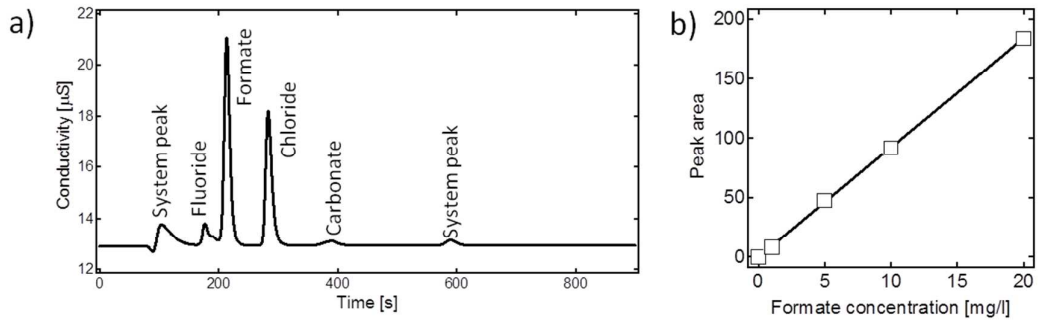

Figure S1 a) *Chromatogram obtained for a standard reaction diluted 100x in pure water* ***b)*** *Calibration curve for formate measured in water-DMF mixture.*

3. Choice of Catalyst, Sacrificial Electron Donor and Photosensitizer

Three different catalysts, $[Ru(bpy)_2(CO)Cl]^+$, $[Ru(bpy)_2(CO)(OCHO)]^+$, and $[Ru(bpy)_2(CO)(H)]^+$, were synthesised with a PF_6 counter anion in accordance with literature procedures. They were found to present the same activity for the production of carbon monoxide and formate. The hydride form was the more convenient catalyst to use due to its greater purity, and the least convenient was the formate form owing to its intrinsic formic acid contamination. The yellow-orange hydridic catalyst, $[Ru(bpy)_2(CO)(H)][PF_6]$, was therefore used in all subsequent studies. Sodium ascorbate was found unsuitable as the electron donor as it exhibited very low productivity for carbon monoxide, and formate analysis was inhibited by the overlapping signal for ascorbate in the ion chromatogram.

Two photosensitizers were studied with both BNAH and TEOA. These were ruthenium trisbipyridine chloride $[Ru(bpy)_3]Cl_2$ and ruthenium tris-4,4'-dimethyl-bipyridine hexafluorophosphate ($[Ru(dm\text{-}bpy)_3](PF_6)_2$). The latter has a more negative reduction potential, *i.e.* the excited state has a higher energy than that of

$[Ru(bpy)_3]^{2+}$, which should result in a stronger driving force for the electron transfer between the photosensitizer and the catalyst. However, the driving force for the electron transfer between the sacrificial electron donor and the photosensitizer is comparably decreased relative to $[Ru(bpy)_3]^{2+}$.

Despite using energetically appropriate electron donors (BNAH) for both sensitizers, a better efficiency was achieved with the conventionally used $[Ru(bpy)_3]Cl_2$, with a significantly greater product yield of ca. 50% for CO and 25% for $HCOO^-$ observed compared to the $([Ru(dm\text{-}bpy)_3](PF_6)_2$. This suggests that the quenching reaction (*i.e.* electron transfer from the sacrificial electron donor) is more limiting in this system than the electron transfer between the photosensitizer and catalyst. The lifetime of the excited sensitizer is less than 1 μs [2], therefore the quenching reaction must be fast to fill the ground state vacancy and avoid radiative deactivation of the photosensitizer.

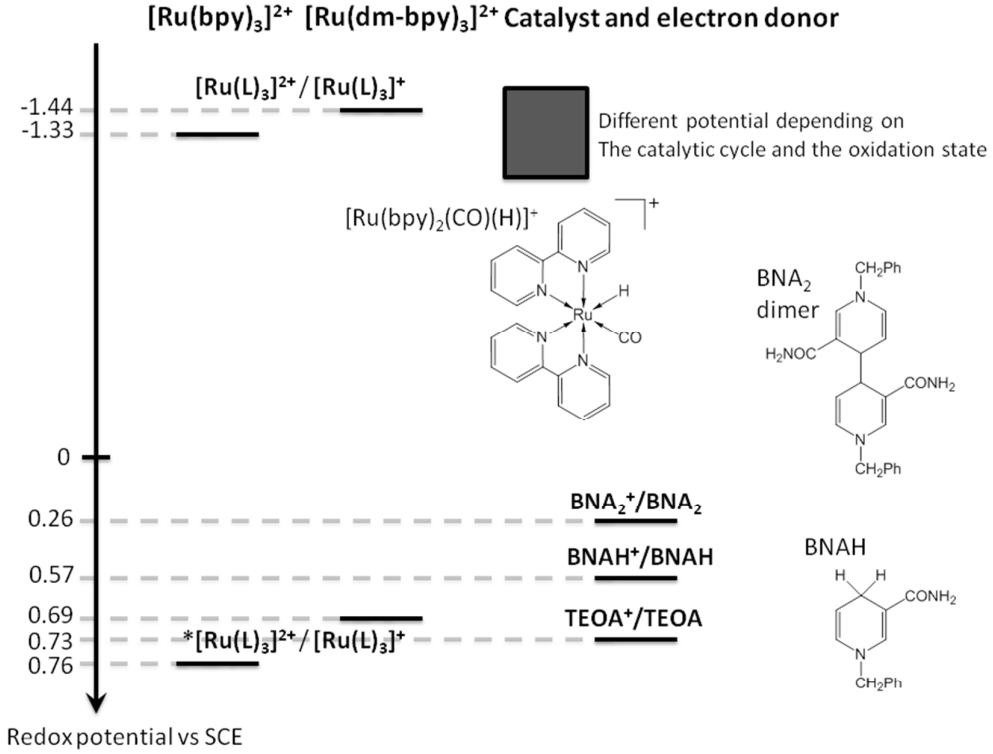

Scheme S2. *Redox potential of the photosensitizers and the electron donor molecules, with the structure of the catalyst, BNAH and* BNA_2

Reactions in water/DMF conducted without a photosensitizer shows that the presence of the photosensitizer is "optional". The catalyst itself is absorbing light, and its excited state can be quenched by BNAH to reduce and activate the catalyst. However, the reaction efficiency is limited, as carbon monoxide production decreased

87% from 200 μmol to 26 μmol, and formate production decreased 50% to 24 μmol. This implies that the catalytic intermediates of the formate cycle (compounds (2) and (4) in Scheme 1), are able to excite photolytically at the bpy ligand and accept an electron from the BNAH directly, whereas the double carbonyl ligand intermediates (complexes (8) and (9), Scheme 1) of the carbon monoxide catalytic cycle are not activated by visible light. UV-vis spectrometry of the catalyst intermediates indicate that the colourless compound, $[Ru(bpy)_2(CO)_2]^{2+}$ is indeed inactive in light above 300 nm wavelength, where as compounds (2) and (4) of the formate catalytic cycle are bright yellow solids[3] with typical Ru-bpy MLCT absorbance peaks in the blue light region (*ca.* 450 nm). Control reaction without light did not produce anything.

4. Mathematic model of BNA_2 limitation

The chain of reactions considered for making a mathematic model of the photosensitisation cycle is presented in scheme S2. Only the photosensitizer cycle has been considered so as to simplify the model and because the catalytic cycle is apparently not rate limiting in the overall process (as shown in Section 3.3).

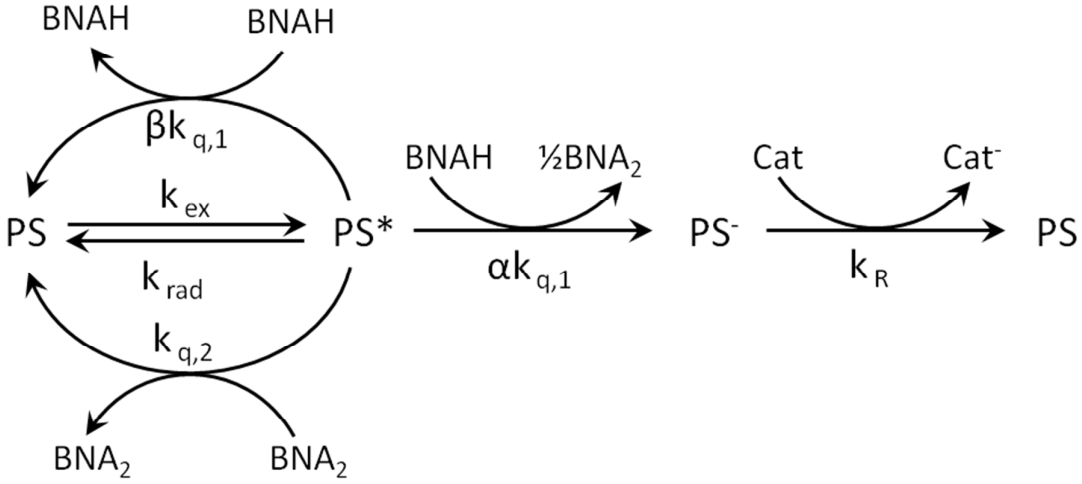

Scheme S3. *Chain of reactions inducing reduction of the catalyst, PS : $[Ru(bpy)_3]^{2+}$, PS* the excited state : $*[Ru(bpy)_3]^{2+}$, and PS⁻ : $[Ru(bpy)_3]^{+}$*

A summary of the constants and terms used in the calculation that correspond to S2 are given below.

- k_{rad} is obtained from the lifetime of the excited state of the photosensitizer reported, τ = 600 ns, $k_{rad} = 1.66*10^6$ [s^{-1}]
- k_{ex} is involved in the initial step of the system, the value will be chosen to fit to the experimental production rate.

- $k_{q,1}$ and $k_{q,2}$ have been reported by Tamaki[4], $k_{q,1} = 1.64*10^7 M^{-1}s^{-1}$ and $k_{q,2} = 3.09*10^8 M^{-1}s^{-1}$. These two quenching rate constants are obtained from the lifetime of the excited state in the presence of the quencher. Due to back electron transfer from the reduced photosensitizer to the oxidized quencher molecule, part of the quenching can be ineffective.
- α factor represents the effective part of the quenching, and β the ineffective quenching due to back electron transfer. For the quenching with BNA_2, the quenching process is supposed to be purely ineffective. This factor is probably the main limitation for the quantum yield during a short time experiment. The maximal quantum yield measured (Φ_{max}=0.2) is taken as an approximation for α.
- As the amount of catalyst is a constant, the k_R[Cat] is replaced by k_R'. The value of k_R' should not be a limitation in the system, as the reaction between PS^- and the catalyst is not in competition with any other. If this reaction is slow there will be an accumulation of PS^- in the reactor.
- The amount of CO_2 reduction product (CO + HCOOH) is equal to the amount of BNA_2 generated

The differential equations dictating evolution of the system are the following:

1. $$\frac{d[PS]}{dt} = -k_{ex}[PS] + k_{rad}[PS^*] + \beta k_{q,1}[BNAH][PS^*] + k_{q,2}[BNA_2][PS^*] + k_R'[PS^-]$$

2. $$\frac{d[PS^*]}{dt} = k_{ex}[PS] - k_{rad}[PS^*] - (\alpha+\beta)k_{q,1}[BNAH][PS^*] - k_{q,2}[BNA_2][PS^*]$$

3. $$\frac{d[BNAH]}{dt} = -\alpha k_{q,1}[BNAH][PS^*]$$

4. $$[PS]_{initial} = [PS] + [PS^*] + [PS^-]$$

5. $$[BNAH]_{initial} = [BNAH] + 1/2[BNA_2]$$

$$\alpha + \beta = 1 \quad with\ 0 \le \alpha \le 1 \qquad\qquad k_R' = k_R[Cat]$$

The two first equations reach a steady state in a very short time (<< 1 second) due to the very short lifetime of the excited state of the photosensitizer. Equation 3 represents the long term consumption of electron donor and generation of CO_2 reduction product (timescale : hours).

The concentration of the different states of the photosensitizer are calculated in the steady state, from equations 1, 2 and 4.

$$[PS^*] = \frac{k_{ex}k_R'}{k_{ex}k_R' + \alpha k_{ex}k_{q,1}[BNAH] + k_R'k_{q,1}[BNAH] + k_R'k_{q,2}[BNA_2] + k_{rad}k_R'}[PS]_{initial}$$

$$[PS^-] = \frac{\alpha k_{ex}k_{q,1}[BNAH]}{k_{ex}k_R' + \alpha k_{ex}k_{q,1}[BNAH] + k_R'k_{q,1}[BNAH] + k_R'k_{q,2}[BNA_2] + k_{rad}k_R'}[PS]_{initial}$$

$$[PS] = [PS]_{initial} - [PS^*] - [PS^-]$$

Using the value of [PS*] obtained, equation 4 is integrated to obtain the decay of BNAH concentration :

$$[BNAH]_t = [BNAH]_{initial}\, e^{(-\alpha k_{q,1}[PS^*]t)}$$

Using the following set of values for the rate constants and initial conditions:

k_{ex}	0.4 s^{-1}
k_{rad}	$1.66*10^6$ s^{-1}
$k_{q,1}$	$1.64*10^7$ $s^{-1}M^{-1}$
$k_{q,2}$	$3.05*10^8$ $s^{-1}M^{-1}$
k_R'	10^9 s^{-1}
α	0.2
β	0.8
$[PS]_{initial}$	$5*10^{-4}$ M
$[BNAH]_{initial}$	0.0625 M

The consumption of BNAH in time can be plotted :

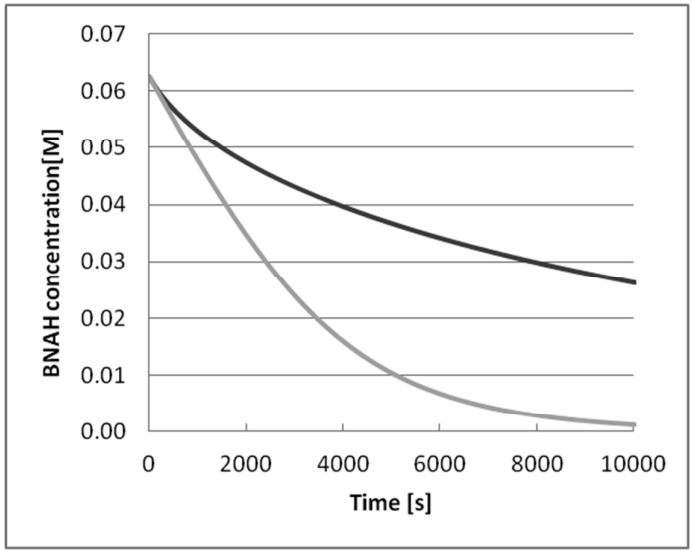

Figure S1. *Decay of BNAH concentration in the reactor, in grey considering only the quenching from BNAH, in dark grey with the inefficient quenching from BNA_2 considered.*

If the quenching by BNA_2 is considered the production rate of system considerably slows down. Due to the faster quenching rate constant with BNA_2, which proves the limitations induced by the increase in BNA_2 concentration in the reactor on the production rate.

The production of BNA_2 calculated by the model can be compared with the amount of reduction product experimentally determined.

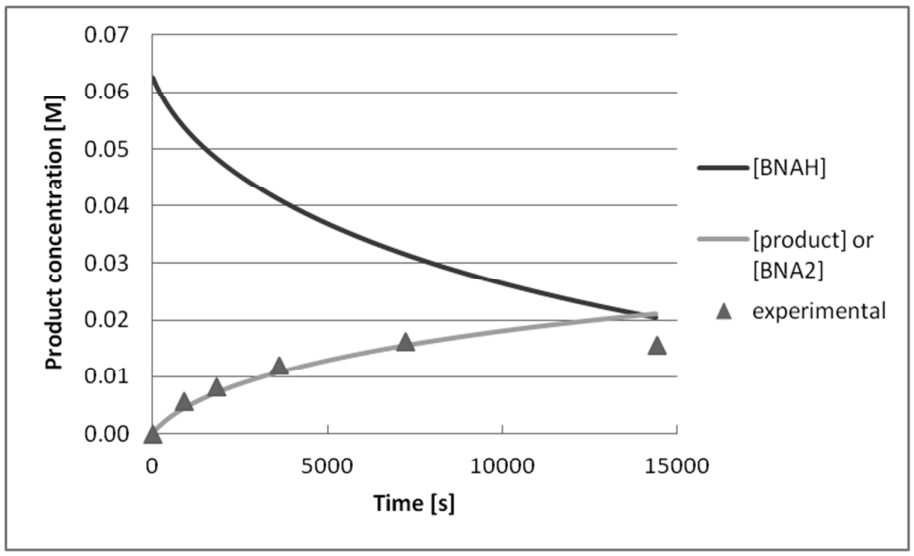

Figure S2. *Comparison of the model with experimental production rate, for conventional high pressure conditions (150 bars, optimized water/DMF ratio, 1 mmol BNAH, 2 µmol catalyst, 8 µmol photosensitizer)*

The correlation with the experimental data is valide, except for the 4 hour experiment where saturation of CO is believed to hinder the catalytic cycle.

The model presented here is considering bulk concentration and production rate, but the concentration of the excited photosensitizer is not equally distributed in the solution. Due to the high light absorption of the solution, almost all the light is absorbed within the first 2 millimetres of solution after the sapphire window. Concentration of PS* is therefore considerably higher in this reduced volume. Diffusion of different species, such as BNAH, BNA_2, CO_2 between the bulk and the window may therefore also limit the reaction rate.

1. Paul, A.; Connolly, D.; Schulz, M.; Pryce, M. T.; Vos, J. G., *Inorg. Chem.* **2012,** *51* (4), 1977-1979.
2. (a) Alstrum-Acevedo, J. H.; Brennaman, M. K.; Meyer, T. J., *Inorg. Chem.* **2005,** *44* (20), 6802-6827; (b) Concepcion, J. J.; House, R. L.; Papanikolas, J. M.; Meyer, T. J., *Proceedings of the National Academy of Sciences* **2012,** *109* (39), 15560-15564.
3. (a) Ooyama, D.; Tomon, T.; Tsuge, K.; Tanaka, K., *J. Organomet. Chem.* **2001,** *619* (2), 299-304; (b) Tanaka, K.; Ooyama, D., *Coord. Chem. Rev.* **2002,** *226* (1-2), 211-218.
4. Tamaki, Y.; Morimoto, T.; Koike, K.; Ishitani, O., *Proc. Natl. Acad. Sci. U. S. A.* **2012,** *109* (Copyright (C) 2012 American Chemical Society (ACS). All Rights Reserved.), 15673-15678, S15673/1-S15673/7.